

## Thermal Transport and Strong Mass Renormalization in $\text{NiCl}_2\text{-4SC}(\text{NH}_2)_2$

Y. Kohama,<sup>1</sup> A. V. Sologubenko,<sup>2</sup> N. R. Dilley,<sup>3</sup> V. S. Zapf,<sup>1</sup> M. Jaime,<sup>1</sup> J. A. Mydosh,<sup>4</sup> A. Paduan-Filho,<sup>5</sup>  
K. A. Al-Hassanieh,<sup>6</sup> P. Sengupta,<sup>7</sup> S. Gangadharaiah,<sup>8,9</sup> A. L. Chernyshev,<sup>8,9</sup> and C. D. Batista<sup>6</sup>

<sup>1</sup>MPA-CMMS, LANL, Los Alamos, New Mexico 87545, USA

<sup>2</sup>II. Physikalisches Institut, Universität zu Köln, Zùlpicher Straße 77, 50937 Köln, Germany

<sup>3</sup>Quantum Design Inc., San Diego, California 92121, USA

<sup>4</sup>Kamerlingh Onnes Laboratory, Leiden University, 2300RA Leiden, The Netherlands

<sup>5</sup>Instituto de Física, Universidade de Sao Paulo, Brazil

<sup>6</sup>Theoretical Division, Los Alamos National Laboratory, Los Alamos, New Mexico 87545, USA

<sup>7</sup>School of Physical and Mathematical Sciences, Nanyang Technological University, 50 Naynag Avenue, Singapore 639798

<sup>8</sup>Department of Physics and Astronomy, University of California, Irvine, California 92697, USA

<sup>9</sup>Max-Planck-Institut für Physik komplexer Systeme, Nöthnitzer Straße 38, 01187 Dresden, Germany  
(Received 19 August 2010; revised manuscript received 2 December 2010; published 18 January 2011)

Several quantum paramagnets exhibit magnetic-field-induced quantum phase transitions to an anti-ferromagnetic state that exists for  $H_{c1} \leq H \leq H_{c2}$ . For some of these compounds, there is a significant asymmetry between the low- and high-field transitions. We present specific heat and thermal conductivity measurements in  $\text{NiCl}_2\text{-4SC}(\text{NH}_2)_2$ , together with calculations which show that the asymmetry is caused by a strong mass renormalization due to quantum fluctuations for  $H \leq H_{c1}$  that are absent for  $H \geq H_{c2}$ . We argue that the enigmatic lack of asymmetry in thermal conductivity is due to a concomitant renormalization of the impurity scattering.

DOI: 10.1103/PhysRevLett.106.037203

PACS numbers: 75.10.Jm, 64.70.Tg, 75.40.Cx

The correspondence between a spin system and a gas of bosons has been very fruitful for describing field-induced ordered phases in a large class of quantum paramagnets [1–4]. In this analogy, a magnetic field  $H$  plays the role of the chemical potential, which, upon reaching a critical value  $H_{c1}$ , induces a  $T = 0$  Bose-Einstein condensation (BEC), provided that the number of bosons is conserved, the kinetic energy is dominant, and the spatial dimension  $d > 1$ . Such a BEC state corresponds to a canted  $XY$  magnetic ordering of the spins.

At the BEC quantum critical point (QCP), the low-energy bosonic excitations have a quadratic dispersion  $\omega = k^2/2m^*$ , where  $m^*$  is the effective mass. This mass is renormalized by quantum fluctuations in the paramagnetic phase  $H \leq H_{c1}$ . In magnets with  $H_{c1} \ll H_{c2}$  the renormalization can be expected to be very strong because of the proximity to the magnetic instability. The transition at  $H_{c1}$  should be contrasted with the second BEC-QCP that takes place at the saturation field  $H_{c2}$  [5]. Since the field-induced magnetization is a conserved quantity, there are no quantum fluctuations and no mass renormalization for the fully polarized phase above  $H_{c2}$ ; i.e., the bare mass  $m$  can be obtained from the single-particle excitation spectrum at  $H \geq H_{c2}$ . Thus, quantum paramagnets are ideal for studying mass renormalization effects because the effective and the bare bosonic masses can be obtained from two different QCPs that occur in the same material.

Here we present theoretical and experimental evidence for a strong mass renormalization effect,  $m/m^* \approx 3$ , in  $\text{NiCl}_2\text{-4SC}(\text{NH}_2)_2$  [referred to as

dichlorotetrakis-thiourea-nickel (DTN)]. We will show that the large asymmetry between the peaks in the low-temperature specific heat,  $C_v(H)$ , in the vicinity of  $H_{c1}$  and  $H_{c2}$  is closely described by analytical and quantum Monte Carlo (QMC) calculations. The mass renormalization also explains similar asymmetries observed in other properties of DTN, such as magnetization [6], electron spin resonance [7], sound velocity [8,9], and magnetostriction [10]. In a remarkable contrast to these properties, peaks in the low-temperature thermal conductivity,  $\kappa$ , near  $H_{c1}$  and  $H_{c2}$  do not show any substantial asymmetry. We provide an explanation to this dichotomy by demonstrating that the leading boson-impurity scattering amplitude is also renormalized by quantum fluctuations, effectively canceling the mass renormalization effect in  $\kappa$ .

DTN is a quantum magnet with tetragonal crystal symmetry that exhibits a field-induced BEC [6,7,11–13] to a very good approximation [14]. The dominant single-ion uniaxial anisotropy  $D = 8.9$  K splits the Ni  $S = 1$  triplet into an  $S^z = 0$  ground state and an  $S^z = \pm 1$  excited doublet. The antiferromagnetic exchange coupling between Ni ions is  $J_c = 2.2$  K along the  $c$  axis and  $J_a = 0.18$  K along the  $a$  and  $b$  axes, while the gyromagnetic factor along the  $c$  axis is  $g = 2.26$  [7]. A magnetic field applied along the  $c$  axis lowers the energy of the  $S^z = 1$  state producing a  $T = 0$  BEC transition at  $H_{c1} = 2.1$  T. The long-range order occurs in a dome-shaped region of the  $T$ - $H$  phase diagram between  $H_{c1}$  and  $H_{c2} = 12.5$  T and below the maximum ordering temperature  $T_{\text{max}} \approx 1.2$  K [11]. The  $T^{3/2}$  dependence of the critical field expected for a

BEC-QCP has been established via direct measurements of the phase boundary with ac susceptibility down to 1 mK [13], and by magnetization measurements [15]. The asymmetry between  $H_{c1}$  and  $H_{c2}$  [6–11] can also be seen directly in the skewed shape of the phase diagram [11].

The Hamiltonian describing the  $S = 1$  spin degrees of freedom of DTN in external field is given by [7]

$$\mathcal{H} = \sum_{\mathbf{r}, \nu} J_{\nu} \mathbf{S}_{\mathbf{r}} \cdot \mathbf{S}_{\mathbf{r}+\mathbf{e}_{\nu}} + D \sum_{\mathbf{r}} (S_{\mathbf{r}}^z)^2 - h \sum_{\mathbf{r}} S_{\mathbf{r}}^z, \quad (1)$$

where  $\mathbf{e}_{\nu}$  are the primitive vectors of the lattice,  $\nu = \{a, b, c\}$ , and  $h = g\mu_B H$ . We introduce Schwinger bosons associated with the fundamental representation of  $SU(3)$  that obey the constraint  $\sum_m b_{\mathbf{r}m}^{\dagger} b_{\mathbf{r}m} = 1$ . The subscript  $m = \{\downarrow, 0, \uparrow\}$  labels the eigenstates of  $S_{\mathbf{r}}^z$  with the eigenvalues  $\{-1, 0, 1\}$ . The spin operators in this representation are

$$S_{\mathbf{r}}^z = n_{\mathbf{r}\downarrow} - n_{\mathbf{r}\uparrow}, \quad S_{\mathbf{r}}^+ = (S_{\mathbf{r}}^-)^{\dagger} = \sqrt{2}(b_{\mathbf{r}\downarrow}^{\dagger} b_{\mathbf{r}0} + b_{\mathbf{r}0}^{\dagger} b_{\mathbf{r}\uparrow}), \quad (2)$$

with  $n_{\mathbf{r}m} = b_{\mathbf{r}m}^{\dagger} b_{\mathbf{r}m}$ . We enforce the constraint by introducing spatially uniform Lagrange multiplier  $\mu$

$$\hat{\mathcal{H}} = \mathcal{H} + \mu \sum_{\mathbf{r}} (b_{\mathbf{r}\downarrow}^{\dagger} b_{\mathbf{r}\downarrow} + b_{\mathbf{r}\uparrow}^{\dagger} b_{\mathbf{r}\uparrow} + b_{\mathbf{r}0}^{\dagger} b_{\mathbf{r}0} - 1). \quad (3)$$

The lowest energy state in the  $H < H_{c1}$  paramagnetic regime is  $b_{\mathbf{r}0}^{\dagger} |0\rangle$  and the ground state corresponds to a nonzero expectation value of the  $S^z = 0$  boson:  $b_{\mathbf{r}0}^{\dagger} = b_{\mathbf{r}0} = s$ . By using the spin representation (2) with the mean-field value for  $b_0^{(\dagger)}$  and neglecting higher-order terms in powers of  $b_{\downarrow(\uparrow)}^{(\dagger)}$ , we obtain the Hamiltonian in the harmonic approximation,  $\hat{\mathcal{H}} = E_0 + \delta \hat{\mathcal{H}}$ :

$$\delta \hat{\mathcal{H}} = \sum_{\mathbf{k}, \sigma} \left[ A_{\mathbf{k}\sigma} \hat{b}_{\mathbf{k}\sigma}^{\dagger} \hat{b}_{\mathbf{k}\sigma} + \frac{B_{\mathbf{k}}}{2} (\hat{b}_{\mathbf{k}\sigma}^{\dagger} \hat{b}_{-\mathbf{k}\bar{\sigma}}^{\dagger} + \text{H.c.}) \right], \quad (4)$$

with  $A_{\mathbf{k}\sigma} = (\mu + s^2 \epsilon_{\mathbf{k}} - h_{\sigma})$  and  $B_{\mathbf{k}} = s^2 \epsilon_{\mathbf{k}}$ , where  $E_0 = N(\mu - D)(s^2 - 1)$  is the bare ground-state energy,  $N$  is the number of sites,  $\sigma = \{\downarrow, \uparrow\}$ ,  $h_{\sigma} = \pm h$ ,  $\bar{\sigma} = -\sigma$ ,  $\hat{b}_{\mathbf{k}\sigma}^{(\dagger)}$  are the Fourier transformed bosonic operators, and  $\epsilon_{\mathbf{k}} = 2 \sum_{\nu} J_{\nu} \cos k_{\nu}$ . The anomalous terms indicate that bosons with opposite  $S^z$  are created and annihilated in the ground state. These are the quantum fluctuations that lead to renormalization of the quasiparticle dispersion relation. The Hamiltonian (4) is diagonalized by

$$\hat{b}_{\mathbf{k}\sigma} = u_{\mathbf{k}} \beta_{\mathbf{k}\sigma} + v_{\mathbf{k}} \beta_{-\mathbf{k}\bar{\sigma}}^{\dagger}, \quad (5)$$

where  $u_{\mathbf{k}} v_{\mathbf{k}} = B_{\mathbf{k}} / 2\omega_{\mathbf{k}}^0$ ,  $u_{\mathbf{k}}^2 + v_{\mathbf{k}}^2 = (\mu + s^2 \epsilon_{\mathbf{k}}) / \omega_{\mathbf{k}}^0$ , and  $\omega_{\mathbf{k}}^0 = \sqrt{\mu^2 + 2\mu s^2 \epsilon_{\mathbf{k}}}$ . The resultant form of  $\hat{\mathcal{H}}$  is

$$\hat{\mathcal{H}} = \tilde{E}_0 + \sum_{\mathbf{k}} [(\omega_{\mathbf{k}}^0 - h) \beta_{\mathbf{k}\downarrow}^{\dagger} \beta_{\mathbf{k}\downarrow} + (\omega_{\mathbf{k}}^0 + h) \beta_{\mathbf{k}\uparrow}^{\dagger} \beta_{\mathbf{k}\uparrow}]. \quad (6)$$

Thus, the low-energy spectrum for  $h < h_{c1}$  is  $\tilde{\omega}_{\mathbf{k}}^< \equiv \omega_{\mathbf{k}}^0 - h$ . The band  $\tilde{\omega}_{\mathbf{k}}^<$  has a minimum at the antiferromagnetic wave vector  $\mathbf{Q} = (\pi, \pi, \pi)$  with the gap  $\Delta^< = \omega_{\mathbf{Q}}^0 - h$ ,

whose vanishing point defines the critical field  $h_{c1} = g\mu_B H_{c1} = \omega_{\mathbf{Q}}^0$ . The ground state energy is also affected by quantum fluctuations

$$\tilde{E}_0 = E_0 + \sum_{\mathbf{k}} (\omega_{\mathbf{k}}^0 - \mu - s^2 \epsilon_{\mathbf{k}}). \quad (7)$$

The saddle point conditions,  $\partial \tilde{E}_0 / \partial s = \partial \tilde{E}_0 / \partial \mu = 0$ , lead to the self-consistent equations for the parameters  $s$  and  $\mu$ ,

$$s^2 = 2 - \frac{1}{N} \sum_{\mathbf{k}} \frac{\mu + s^2 \epsilon_{\mathbf{k}}}{\omega_{\mathbf{k}}^0}, \quad D = \mu + \frac{\mu}{N} \sum_{\mathbf{k}} \frac{\epsilon_{\mathbf{k}}}{\omega_{\mathbf{k}}^0}. \quad (8)$$

Using parameters for DTN given in Ref. [7], the resulting values are  $s^2 = 0.92$  and  $\mu = 10.3$  K.

This low-energy theory is valid only for  $H \leq H_{c1}$ . For  $H \geq H_{c2}$  spins are fully polarized and the spectrum can be computed exactly. Since there are no quantum fluctuations for  $H \geq H_{c2}$ , the exact value of  $h_{c2}$  is  $h_{c2} = g\mu_B H_{c2} = D - 2\epsilon_{\mathbf{Q}}$ , while the unrenormalized excitation spectrum is  $\tilde{\omega}_{\mathbf{k}}^> \equiv \epsilon_{\mathbf{k}} - \epsilon_{\mathbf{Q}} + h - h_{c2}$ , which also has a minimum at  $\mathbf{Q}$  with the gap  $\Delta^> = h - h_{c2}$ . Since only the excitations near  $\mathbf{k} = \mathbf{Q}$  are important at low temperatures, we define the mass tensors for  $H < H_{c1}$  and  $H > H_{c2}$  as

$$\frac{1}{m_{\nu\nu}^*} = \left. \frac{\partial^2 \tilde{\omega}_{\mathbf{k}}^<}{\partial k_{\nu}^2} \right|_{\mathbf{k}=\mathbf{Q}}, \quad \frac{1}{m_{\nu\nu}^*} = \left. \frac{\partial^2 \tilde{\omega}_{\mathbf{k}}^>}{\partial k_{\nu}^2} \right|_{\mathbf{k}=\mathbf{Q}}. \quad (9)$$

Then the mass renormalization factor is given by

$$\frac{m_{\nu\nu}}{m_{\nu\nu}^*} = s^2 \frac{\mu}{\omega_{\mathbf{Q}}^0} \approx \frac{H_{c2}}{4H_{c1}} \cdot \left( 1 + \sqrt{1 + \frac{8H_{c1}^2}{H_{c2}^2}} \right). \quad (10)$$

For the parameters from Ref. [7], we obtain  $m_{\nu\nu} / m_{\nu\nu}^* \approx 3.2$ . Such a large difference of masses must readily demonstrate itself in the strong asymmetry of the  $C_{\nu}$  vs  $H$  curves near  $H_{c1}$  and  $H_{c2}$  as well as in the slopes of the specific heat dependence on  $T$  at the critical fields where  $C_{\nu} \propto (Tm)^{3/2}$ . These theoretical expectations are supported by the experimental  $C_{\nu}(T, H)$  data shown in Figs. 1 and 2.

The  $C_p$  was measured in single crystals of DTN grown from aqueous solutions of thiourea and nickel chloride, with magnetic field applied along the crystalline  $c$  axis. The experimental  $C_p$  vs  $H$  was obtained using an ac technique [16], while sweeping the magnetic field in a  $^3\text{He}$  fridge furnished with a 17 T superconducting magnet system at the National High Magnetic Field Laboratory and the Los Alamos National Laboratory. We also used the standard thermal relaxation method to obtain  $C_{\nu}$  vs  $T$  with a dilution refrigerator in a 16 T Physical Properties Measurement System at Quantum Design, Inc. A strongly asymmetric  $C_p$  vs  $H$  is shown in Fig. 1 for fixed temperatures  $T = 0.75$  K (green line) and  $T = 0.4$  K (red line), alongside the results of the QMC simulations of the spin Hamiltonian in Eq. (1) in a  $8 \times 8 \times 32$  lattice (solid symbols). The agreement between the QMC results and the experimental data is very good. For the lowest temperature,

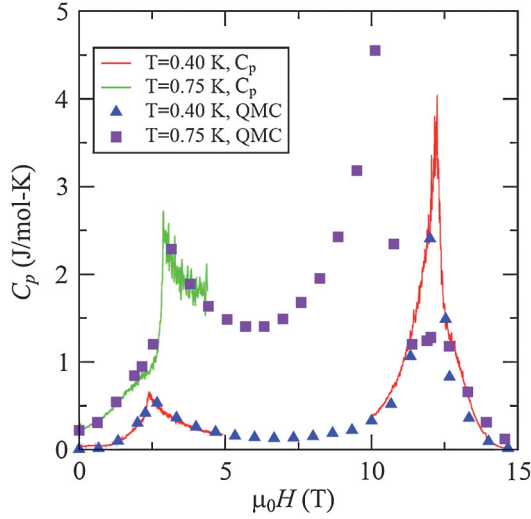


FIG. 1 (color). Specific heat as a function of magnetic field for two temperatures. Measurements and QMC simulations were also performed at other temperatures showing nearly perfect agreement and the same characteristic behavior of  $C_p$  vs  $H$ .

the asymmetry of the peaks is  $C_{p2}/C_{p1} \approx 6$ , close to  $(m/m^*)^{3/2} \approx 5.7$  expected from the theory above.

Our  $C_v$  vs  $T$  experimental data close to  $H_{c1}$  (top panel) and  $H_{c2}$  (bottom panel) are displayed in Fig. 2 (lines with symbols). The results of the QMC simulations of Eq. (1) at  $H_{c1}$  and  $H_{c2}$  are shown by the solid lines. The dashed lines correspond to the analytical calculation of  $C_v(T)$  for a dilute gas of hardcore bosons [Eq. (6)] that have the spectra given by  $\tilde{\omega}_{\mathbf{k}}^-$  and  $\tilde{\omega}_{\mathbf{k}}^+$  at  $H_{c1}$  and  $H_{c2}$ . The on-site boson-boson repulsion is taken into account at the mean-field level by summing the ladder diagrams (see Ref. [3]). Since this approach is only valid for low density of bosons,

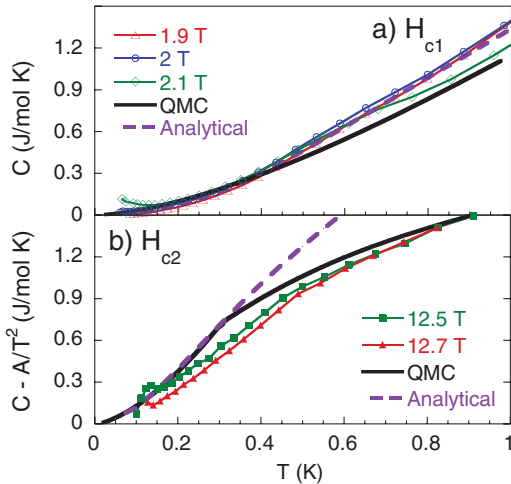


FIG. 2 (color). Specific heat data as a function of  $T$  for magnetic fields near (a)  $H_{c1}$  and (b)  $H_{c2}$ . A Schottky anomaly tail,  $A/T^2$  with  $A = 0.018$  J/molK<sup>3</sup>, has been subtracted for fields near  $H_{c2}$ . The full lines correspond to QMC simulations of Eq. (1) for  $H = H_{c1(2)}$  and the parameters of Ref. [7]. The dashed lines are analytical calculations.

it agrees closely with the QMC results at low  $T$ , but deviates from them at higher temperatures. The very good agreement between the theoretical results and the experimental curves at  $H_{c1}$  and  $H_{c2}$  confirms quantitatively the expected mass renormalization for  $H \leq H_{c1}$ .

The thermal conductivity was measured in DTN single crystals using the standard uniaxial heat flow method, where the temperature difference was produced by a heater attached to one end of the sample and monitored with a matched pair of RuO<sub>2</sub> thermometers. The heat flow and the magnetic field were parallel to the  $c$  axis. Similar observations were reported in Ref. [17] although their data at base temperature (380 mK) do not agree with ours, measured down to 300 mK.

The lighter mass of bosons for  $H \leq H_{c1}$  implies not only large asymmetry between the peaks in the specific heat field dependence, but also similar asymmetries in a number of other properties of DTN [6–10], all exhibiting a much stronger anomaly at  $H_{c2}$  than at  $H_{c1}$ . In contrast, the low-temperature thermal conductivity does not show any substantial asymmetry between the  $H_{c1}$  and  $H_{c2}$  data. Figure 3 shows the field dependence of the thermal conductivity,  $\kappa$ , normalized to the  $H = 0$  value,  $\kappa(0)$ , for several low values of  $T$ . Since the  $H = 0$  magnetic excitation spectrum has a gap of about 3 K [7], only phonons contribute to  $\kappa(0)$  at low temperatures. The behavior of  $\kappa$  changes qualitatively in the field because the gap is closed between  $H_{c1}$  and  $H_{c2}$ . The low-temperature magnetic excitations provide a substantial contribution to the thermal conductivity as is clear from  $\kappa(H)/\kappa(0)$  being  $>1$  in Fig. 3. Here we focus on the low-temperature behavior of  $\kappa$  at the critical points  $H_{c1}$  and  $H_{c2}$ . A detailed analysis of the other aspects of  $\kappa$  will be provided elsewhere [18].

At low enough temperatures, scattering of bosons on each other should diminish and the leading scattering in this regime should be due to defects. In the second Born

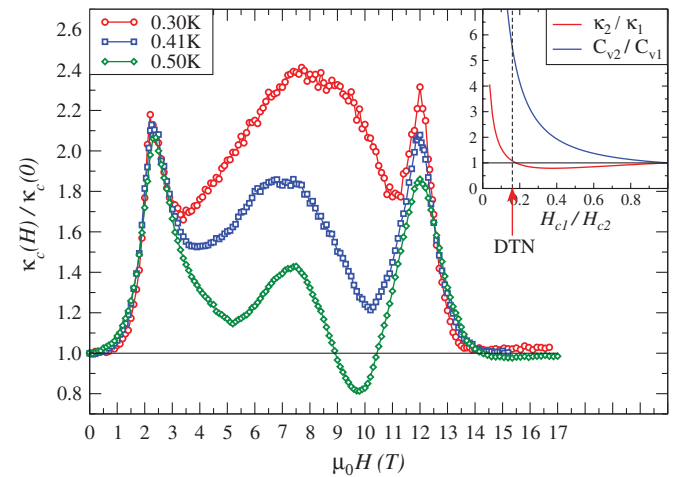


FIG. 3 (color). Thermal conductivity of DTN along the  $c$  axis as a function of  $H$  for three different temperatures. Inset: Theoretical prediction for the peak ratios  $\kappa_2/\kappa_1$  and  $C_{v2}/C_{v1}$  vs  $H_{c1}/H_{c2}$ .

approximation, the disorder-averaged inverse mean-free path of an excitation of mass  $m$  due to scattering on point-like impurities is [19]

$$\ell^{-1} = \frac{n_i}{2\pi} |V|^2 m^2, \quad (11)$$

where  $n_i$  is the impurity concentration and  $V$  is the effective impurity potential. When the excitation gap vanishes at  $H_{c1}$  or  $H_{c2}$ , thermal conductivity at low  $T$  can be written as

$$\kappa \propto \frac{\ell}{m} \int_0^{\sqrt{mT}} k^3 dk \propto mT^2 \ell \propto \frac{T^2}{n_i m |V|^2}. \quad (12)$$

The theoretical temperature dependence,  $\kappa \propto T^2$ , is in a good agreement with the measured low  $T$  thermal conductivity. However, this does not shed any light on the lack of asymmetry between the peaks. Since vacancies or substitutional impurities are expected to be rare in clean systems like DTN, we can assume that random lattice distortions are the most common source of disorder. Because  $D$  is the largest parameter in Eq. (1), the most significant effect of these distortions is a real space modulation of  $D$

$$\mathcal{H}_{\text{imp}}^D = \delta D (S_i^z)^2 \Rightarrow \delta D \sum_{\sigma, \mathbf{k}, \mathbf{k}'} e^{i\mathbf{R}_i(\mathbf{k}-\mathbf{k}')} b_{\mathbf{k}\sigma}^\dagger b_{\mathbf{k}'\sigma}, \quad (13)$$

where  $\mathbf{i}$  is the impurity site and we used the mapping (2).

This is where the renormalization due to quantum fluctuations becomes crucial again. For  $H = H_{c2}$  the impurity scattering in (13) is not renormalized and  $V_2 \equiv \delta D$ . On the other hand, for  $H = H_{c1}$  the scattering is affected by the quantum fluctuations. Since the dressed bosonic excitations are related to the bare ones through Eq. (5), this transforms impurity scattering (13) into [ $\mathbf{R}_i = 0$ ]

$$\mathcal{H}_{\text{imp}}^D = \delta D \sum_{\sigma, \mathbf{k}, \mathbf{k}'} (u_{\mathbf{k}} u_{\mathbf{k}'} + v_{\mathbf{k}} v_{\mathbf{k}'}) \beta_{\mathbf{k}\sigma}^\dagger \beta_{\mathbf{k}'\sigma}. \quad (14)$$

Thus, the impurity potential at  $H_{c1}$  is  $V_1 = \delta D (u_{\mathbf{Q}}^2 + v_{\mathbf{Q}}^2)$ , which will modify the mean-free path in (11). After some algebra utilizing Eqs. (12), (5), and (10), we finally obtain

$$\frac{\kappa_2}{\kappa_1} = \frac{m\ell_2}{m^*\ell_1} = \left(\frac{m}{m^*}\right) \frac{1}{4s^4} \left[1 + s^4 \left(\frac{m^*}{m}\right)^2\right]^2. \quad (15)$$

This expression contains a large prefactor ( $m/m^*$ ) coming from the renormalization of the density of states and velocity in (12), and would formally imply a larger peak at  $H_{c2}$ , similar to the specific heat and other quantities. However, this effect is partially compensated by the numerical factor  $\approx 1/4 + O((m^*/m)^2)$ , which comes from the renormalization of the mean-free path. By using the DTN parameters, we obtain  $\kappa_2/\kappa_1 \approx 1.1$  in an excellent agreement with the data in Fig. 3. Thus, the mass renormalization effect in thermal conductivity is compensated by a similar renormalization effect in the impurity scattering. To show that this is not a mere coincidence, we provide our prediction for the  $H_{c1}/H_{c2}$  dependence of the peak ratios in thermal conductivity  $\kappa_2/\kappa_1$  and specific heat  $C_{v2}/C_{v1}$  on  $H_{c1}/H_{c2}$  [see inset in Fig. 3]. Here we used the relation between

the mass ratio and  $H_{c1}/H_{c2}$  given by Eq. (10). The vertical line corresponds to the DTN value of  $H_{c1}/H_{c2} \approx 0.17$ . It is remarkable that  $\kappa_2/\kappa_1$  and  $C_{v2}/C_{v1}$  behave in very different ways. In particular,  $\kappa_2/\kappa_1 \approx 1$  while the peaks in  $C_v$  are very asymmetric for  $0.1 \leq H_{c1}/H_{c2} \leq 1$ . With this insight, we also suggest an experimental verification of our theory by conducting the heat conductivity measurement in DTN under pressure. A modest decrease of  $H_{c1}$  by 1 T should lead to an increase in  $\kappa_2/\kappa_1$  by a factor of 2.

The leading impurity scattering (13) and the resulting expression for the ratio  $\kappa_2/\kappa_1$  in (15) will remain valid for the other BEC magnets even though they may not be dominated by the single-ion anisotropy term. For instance, in the dimer-based systems [4], the disorder in the leading intradimer coupling translates into the local modulation of the chemical potential which is equivalent to our Eq. (13). Thus, our Eq. (15) can be verified in other BEC compounds.

In conclusion, by using the example of DTN, we connected the asymmetry in the physical properties of BEC magnets with the mass renormalization of the elementary excitations due to quantum fluctuations of the paramagnetic state. We also resolved the enigmatic absence of this asymmetry in the low- $T$  thermal conductivity by identifying the leading scattering mechanism and by demonstrating that the renormalization of the latter compensates the mass renormalization effect.

This work was supported by the NSF, the State of Florida, the U.S. DOE under Grant No. DE-FG02-04ER46174 (A. L. C.) and by the DFG, SFB 608 (A. S. and J. M.).

- 
- [1] I. Affleck, *Phys. Rev. B* **43**, 3215 (1991).
  - [2] T. Giamarchi and A. M. Tsvelik, *Phys. Rev. B* **59**, 11398 (1999).
  - [3] T. Nikuni *et al.*, *Phys. Rev. Lett.* **84**, 5868 (2000).
  - [4] M. Jaime *et al.*, *Phys. Rev. Lett.* **93**, 087203 (2004).
  - [5] E. G. Batyev and L. S. Braginskii, *Sov. Phys. JETP* **60**, 781 (1984).
  - [6] A. Paduan-Filho, X. Gratens, and N.F. Oliveira, *Phys. Rev. B* **69**, 020405(R) (2004).
  - [7] S. A. Zvyagin *et al.*, *Phys. Rev. Lett.* **98**, 047205 (2007).
  - [8] O. Chiatti *et al.*, *J. Phys. A* **150**, 042016 (2009).
  - [9] S. Zherlitsyn *et al.*, *J. Phys. A* **145**, 012069 (2009).
  - [10] V. S. Zapf *et al.*, *Phys. Rev. B* **77**, 020404(R) (2008).
  - [11] V. S. Zapf *et al.*, *Phys. Rev. Lett.* **96**, 077204 (2006).
  - [12] S. A. Zvyagin *et al.*, *Phys. Rev. Lett.* **B 77**, 092413 (2008).
  - [13] L. Yin *et al.*, *Phys. Rev. Lett.* **101**, 187205 (2008).
  - [14] The number of bosons is never strictly conserved in real magnets due to spin-orbit interaction.
  - [15] A. Paduan-Filho *et al.*, *Phys. Rev. Lett.* **102**, 077204 (2009).
  - [16] Y. Kohama *et al.*, *Rev. Sci. Instrum.*, **81** 104902 (2010).
  - [17] X. F. Sun *et al.*, *Phys. Rev. Lett.* **102**, 167202 (2009).
  - [18] A. L. Chernyshev and C. D. Batista (unpublished).
  - [19] G. D. Mahan, *Many-Particle Physics* (Plenum Press, New York, London, 1990).